Development 137, 2659-2669 (2010) doi:10.1242/dev.049791

Full-term mouse development by abolishing Zn^{2+}-dependent metaphase II arrest without Ca^{2+} release

Toru Suzuki*, Naoko Yoshida, Emi Suzuki, Erina Okuda and Anthony C. F. Perry*,†

SUMMARY

In vertebrates, a rise in intracellular free Ca^{2+} (Ca^{2+}_i) levels during fertilization initiates second metaphase (mII) exit and the developmental programme. The Ca^{2+} rise has long been considered to be crucial for development, but verifying this contribution would benefit from defining its role during fertilization. Here, we delineate the role of Ca^{2+} release during mII exit in wild-type mouse eggs and show that it is dispensable for full-term development. Exit from mII can be induced by Zn^{2+}-specific sequestration without Ca^{2+} release, eliciting Cyclin B degradation in a manner dependent upon the proteasome pathway and intact microtubules, but not accompanied by degradation of the meiotic regulator Emi2. Parthenogenotes generated by Zn^{2+} sequestration developed in vitro with normal expression of Ca^{2+}-sensitive genes. Meiotic exit induced by either Ca^{2+} oscillations or a single Ca^{2+} rise in oocytes containing a signaling-deficient sperm resulted in comparable developmental rates. In the absence of Ca^{2+} release, full-term development occurred ~50% less efficiently, but at readily detectable rates, with the birth of 27 offspring. These results show in intact mouse oocytes that Zn^{2+} is essential for mII arrest and suggest that triggering meiotic exit is the sole indispensable developmental role of Ca^{2+} signaling in mammalian fertilization.

KEY WORDS: Metaphase II exit, Ca^{2+}, Mouse, Zn^{2+}

INTRODUCTION

Fertilizable vertebrate oocytes are typically arrested in the second meiotic metaphase (mII) by the cytostatic factor Emi2, which sustains mII until fertilization by preventing the anaphase promoting complex (APC) E3 ubiquitin ligase from associating productively with its co-activator, Cdc20 (Stricker, 1999; Schmidt et al., 2005; Peters, 2006; Shoji et al., 2006). The principal effect of this association is to impede the ubiquitylation and consequent proteasomal destruction of the separase inhibitor securin and of cyclin B (CycB), an essential component of maturation promoting factor (MPF), which is responsible for mII arrest (Gautier et al., 1990; Peters, 2002; Peters, 2006). Thus, Emi2 sustains mII by stabilizing CycB, and, in *Xenopus*, is itself removed following Ca^{2+}-dependent ubiquitylation by the Skp-Cullin-Fbox E3 ubiquitin ligase SCF^{Trcpb} (Tung et al., 2005). A model of the Emi2 regulatory network is presented elsewhere (Perry and Verlhac, 2008).

Emi2 possesses a functional paralogue, Emi1, that prevents premature APC activation in early mitosis (Reimann et al., 2001a). Emi1 inhibits APC activity via separable APC- and IBR/TRIAD/C6HC Zn^{2+}-binding domains resembling the Emi2 C terminus; mutation of the Emi1 zinc-binding region (ZBR) converts Emi1 into an APC substrate (Schmidt et al., 2005; Miller et al., 2006). A single ZBR mutant of *Xenopus* Emi2 lacks cytostatic activity in cell-free extracts, but its stability has not been reported (Schmidt et al., 2005).

Laboratory of Mammalian Molecular Embryology, RIKEN Center for Developmental Biology, 2-2-3 Minatojima Minamimachi, Chuo-ku, Kobe 650-0047 Japan.

*Present address: Laboratory of Mammalian Molecular Embryology, Centre for Regenerative Medicine, University of Bath, Bath BA2 7AY, UK
†Author for correspondence (perry135@aol.com)

Accepted 10 May 2010

Fertilization in metazoans is characterized by Ca^{2+} release from inositol 1,4,5-trisphosphate [IP_3; Ins(1,4,5)P_3] receptor-sensitive oocyte stores to enable cytoplasmic signaling (Mazia, 1937; Whitaker and Irvine, 1984; Miyazaki et al., 1992) (for a review, see Runft et al., 2002). The resultant increase in intracytoplasmic 'free' Ca^{2+} (Ca^{2+}_i) concentration is considered to be a universal requisite among animals for initiating both meiotic exit and the events of oocyte activation that presage full-term development (Runft et al., 2002; Yanagimachi, 1994; Ducibella and Fissore, 2008). Sperm-oocyte union at fertilization in *Xenopus* induces a single [Ca^{2+}_i] rise lasting 5 minutes (Kline and Nuccitelli, 1985; Runft et al., 2002). In the mouse, a relatively large initial [Ca^{2+}_i] increase is followed by oscillatory increases that spike every 5-15 minutes until pronucleus formation ~4 hours later (Igusa et al., 1983; Cuthbertson and Cobbold, 1985; Runft et al., 2002).

Ca^{2+} signaling in *Xenopus* fertilization results in phosphorylation of Emi2 to target it for Plk1-mediated phosphorylation and proteolysis, and hence relieve mII arrest (Lorca et al., 1993; Runft et al., 2002; Rauh et al., 2005; Schmidt et al., 2005). This signal is relayed in diverse species via the Ca^{2+}-dependent kinase, calmodulin kinase II (CaMKII) (Lorca et al., 1993); injection of mouse mII oocytes with cRNA encoding constitutively active CaMKII results in meiotic progression (Knott et al., 2006) and native CaMKII activity in newly fertilized mouse eggs shadows [Ca^{2+}_i] oscillations (Markoulaki et al., 2004). Moreover, the events of oocyte activation are impaired by depleting the γ isoform of CaMKII (CaMKIIγ) or prevented in animals carrying a targeted deletion of the CaMKIIγ gene (*Camk2g*) (Chang et al., 2009; Backs et al., 2010). The roles of Ca^{2+} release and CaMKIIγ are different in oocyte activation in that CaMKIIγ is not directly required for cortical granule exocytosis or maternal mRNA recruitment. However, both these processes do require Ca^{2+} release and/or meiotic progression (Backs et al., 2010).

A large and growing body of evidence links the $[Ca^{2+}_i]$ change at fertilization to early mammalian development (Runft et al., 2002; Ducibella and Fissore, 2008). Blocking $[Ca^{2+}_i]$ increase prevents mouse mII exit in response to oocyte-activating stimuli (Kline and Kline, 1992) and discrete activation events are driven by differential responses to $[Ca^{2+}_i]$ oscillation number and the sum of their duration (Ducibella et al., 2002; Ozil et al., 2005). Fertilization-induced $[Ca^{2+}_i]$ elevation also regulates key downstream processes (Rogers et al., 2006; Ozil et al., 2006; Ducibella and Fissore, 2008). The absence or premature termination of $[Ca^{2+}_i]$ oscillations causes marked downregulation of genes expressed at the eight-cell and blastocyst stages (Rogers et al., 2006), while stimulating $[Ca^{2+}_i]$ oscillation frequency by electrical hyperstimulation causes upregulation of (fewer) genes; both affected peri- and post-implantation development (Ozil et al., 2006). Thus, there is evidence of short- and long-term developmental roles for Ca^{2+}_i mobilization during mammalian fertilization and it is possible that this reflects a requirement for CaMKIIγ activity. Activation of the Ca^{2+}-dependent protein phosphatase calcineurin (PP2B) is essential for mII exit in *Xenopus* (Mochida and Hunt, 2007; Nishiyama et al., 2007), raising the possibility of additional mouse oocyte activation pathways with downstream developmental roles. The study of these pathways would benefit from isolating the role of Ca^{2+} release per se during fertilization.

We explored this possibility as part of our interest in signaling in mII exit and here report that Zn^{2+} is essential for mouse mII arrest: Zn^{2+} depletion induces Ca^{2+}-independent mII exit without Ca^{2+} release. We harnessed this observation to explore the developmental role of fertilization-induced Ca^{2+} release and show that, in the presence of a paternal genome, oscillatory, monotonic or zero Ca^{2+} rises can support healthy full-term development. This work introduces a pivotal cellular role for Zn^{2+} in meiotic homeostasis and suggests that the sole indispensable developmental role of fertilization-induced Ca^{2+}_i release is to induce mII exit.

MATERIALS AND METHODS

Collection, culture and activation of oocytes

Mice were supplied by SLC (Shizuoka-ken, Japan) and handled according to institutional guidelines. Eight- to 12-week-old B6D2F$_1$ females were superovulated using standard serial intraperitoneal injections of pregnant mare serum gonadotropin (PMSG) followed 48 hours later by human chorionic gonadotropin (hCG). Oviductal metaphase II (mII) oocytes were collected typically 12 to 15 hours post-hCG injection and cumulus cells removed following hyaluronidase treatment as previously described (Yoshida et al., 2007a).

'Conventional' activation of mII oocytes was with $SrCl_2$ or ethanol. For $SrCl_2$ activation, oocytes were incubated in Ca^{2+}-free CZB (Chatot et al., 1989) supplemented with 10 mM $SrCl_2$ in humidified CO_2 [5% (v/v) in air] at 37°C for 1 to 6 hours. Oocytes were washed in KSOM and incubation continued at 37°C. Activation with 7% (v/v) ethanol in HEPES-buffered CZB (CZBH) was at room temperature for 5 minutes, after which oocytes were washed in KSOM and incubated in humidified CO_2 [5% (v/v) in air] at 37°C. Activation by exposure to *N,N,N′,N′*-tetrakis-(2-pyridylmethyl)-ethylenediamine (TPEN; Sigma-Aldrich, MO, USA) was for 45 minutes in KSOM containing TPEN at the concentration indicated (typically 100 μM), in humidified CO_2 [5% (v/v) in air] at 37°C. Following TPEN treatment, oocytes were washed in KSOM (three or four times), then either incubated in KSOM or subjected to imaging to determine relative $[Ca^{2+}_i]$; the period between TPEN wash-out and the initiation of imaging was 60 to 120 seconds. In the experiments shown in Fig. 3D, cRNA-injected mII oocytes were exposed to TPEN for 45 minutes and then to ethanol, as described above. Where appropriate, oocytes were incubated in nocodazole (Sigma) for 1.5 hours before exposure to 10 mM $SrCl_2$ or 100 μM TPEN for 1 hour, and washing and continued incubation in KSOM for 6 hours.

To obtain diploid parthenogenotes, activation media and KSOM for subsequent incubations were supplemented with 5 μg/ml cytochalasin B (MP Biomedicals LLC, OH, USA) for 6 hours from the initiation of activation. Parthenogenotes were then washed and incubated in KSOM lacking cytochalasin B.

Transition metal ion chelation and rescue assays

To assess the effect on mII oocytes of treatment with TPEN, we selected those whose Pb_1 had degraded so that Pb_2 extrusion could be visualized more clearly. Oocytes collected 12-15 hours post-hCG were placed in KSOM containing TPEN. TPEN exhibits the following K_ds for divalent transition metal ions specifically assessed in this work: Zn^{2+}, $10^{15.58}$ M^{-1}; Fe^{2+}, $10^{14.61}$ M^{-1}; Cu^{2+}, 10^{20} M^{-1}; Mn^{2+}, $10^{10.27}$ M^{-1}. Binding constants for TPEN and other transition metal ion-binding reagents used here are shown in Table S1 in the supplementary material. TPEN was stored in aliquots at –20°C as a 10 mM stock solution in DMSO and freshly diluted in KSOM immediately prior to incubation. Oocytes were typically examined for Pb_2 extrusion 90 minutes after TPEN exposure. In some experiments, oocytes had been injected with cRNAs 4-5 hours prior to KSOM/TPEN incubation. Where appropriate, TPEN-containing media was supplemented with 10 μM epoxomycin (Biomol International, PA, USA) or 20 μM Z-LLL-CHO (Peptide Institute, Saito, Japan), which are (respectively) irreversible and reversible proteasome inhibitors. Transition metal ion rescue assays were performed either in parallel with, or sequential to, TPEN incubation. For rescue in parallel, oocytes lacking a Pb_1 were incubated for 1.5 hours in KSOM containing 100 μM TPEN together with 100 μM $ZnSO_4$ (Zn^{2+}), $MnSO_4$ (Mn^{2+}), $CuSO_4$ (Cu^{2+}) or $FeSO_4$ (Fe^{2+}), as appropriate. Oocytes were then washed in KSOM and scored for Pb_2 extrusion 1.5 hours later. For sequential rescue, oocytes were cultured for 2 hours in KSOM containing 100 μM TPEN plus 20 μM Z-LLL-CHO, washed in KSOM/20 μM Z-LLL-CHO alone (to remove TPEN) and transferred to KSOM/20 μM Z-LLL-CHO supplemented with 100 μM $ZnSO_4$ (Zn^{2+}), $MnSO_4$ (Mn^{2+}), $CuSO_4$ (Cu^{2+}), $FeSO_4$ (Fe^{2+}), $NiSO_4$ (Ni^{2+}) or $CoSO_4$ (Co^{2+}), as appropriate and incubated for 1 hour before washing and continuing the culture for 3 hours in KSOM alone. Scoring was of Pb_2 extrusion. To determine the effect of chelating non-Zn^{2+} transition metal ions, mII oocytes were incubated for 1.5 to 3.0 hours in KSOM containing 100 μM *p*-aminosalicylic acid (MP Biomedicals, CA, USA) for Mn^{2+} chelation, or ammonium tetrathiomolybdate (Sigma) for Cu^{2+} chelation or 2,2′-bipyridine (2,2′-dipyridyl; Sigma) for Fe^{2+} chelation. Meiotic progression was scored by the appearance of a Pb_2.

Preparation and injection of cRNA and siRNA

Cloning Emi2 to generate cRNA-encoded mCherry fusions has been described elsewhere (Shoji et al., 2006). Mouse Cyclin B1 with a C-terminal Venus fusion was generated by inserting an *Xho*I-*Xba*I *Venus* fragment into plasmid pCI-neo (Promega Corp., WI, USA). A Cyclin B1 PCR product was inserted into this construct [using primers (5′ to 3′): CTAGCTAGCACCATGGCGCTCAGGGTCAC and CTGCTCGAGCC-ATGCCTTTGTCACGGCC] as an *Nhe*I-*Xho*I fragment.

cRNAs were synthesized in vitro from linear plasmid DNA template and 5′-capped and polyadenylated in the same reaction using an mSCRIPT^{TM} mRNA Production System (Epicentre Biotechnologies, WI, USA) according to the manufacturer's instructions. cRNAs were dissolved in nuclease-free distilled water, quantified and stored in aliquots at –80°C. Double-stranded siRNAs (iGENE Therapeutics, Tsukuba, Japan) were designed as described previously (Shoji et al., 2006) and stored in aliquots at –80°C.

RNA solutions were diluted with sterile PBS to the desired concentration and injected (typically at concentrations of 0.5 to 1 mg/ml for cRNA and 25 μM for siRNA) within 1 hour of thawing via a piezo-actuated micropipette (tip inner diameter 6~7 μm) into mII oocytes in M2 medium. Oocytes were cultured for 4 or 7 hours following injection of cRNA or siRNA respectively, and, where appropriate, then transferred to KSOM containing TPEN.

Imaging relative [Ca^{2+}_i] and available [Zn^{2+}]

Indirect imaging to determine relative [Ca^{2+}_i] within mII oocytes and following 500 μM IP_3 injection, ICSI, ethanol treatment, $SrCl_2$ treatment and/or TPEN treatment was as described previously (Yoshida et al., 2007a). Injection and analysis of mII oocytes was ~18-20 hours after hCG injection. Oocytes were loaded for 30 minutes with 5 μM fura 2 acetoxymethyl ester (Fura 2-AM; Molecular Probes, CA, USA) before exposing them to the activating stimulus. Fluorescence recordings were then initiated immediately, as previously described (Yoshida et al., 2007a), and processed with AQUA COSMOS ratio imaging application software (Hamamatsu Photonics, Japan). For experiments with TPEN, recordings typically started 60-120 seconds after TPEN wash out. In some experiments, TPEN-treated oocytes (n=17) were quickly washed and transferred to a juxtaposed drop on the microscope stage for immediate imaging, with an interval of ~30 seconds between washing and recording.

To determine the effect of Ca^{2+}_i chelation on activation stimuli, oocytes were incubated in the plasma membrane permeant Ca^{2+} sponge 1,2-bis-(o-aminophenoxy)-ethane-*N,N,N′,N′*-tetraacetic acid tetraacetoxymethyl ester (BAPTA-AM) (Calbiochem, EMD Chemicals, Gibbstown, NJ, USA) at 50 μM in KSOM for 20 minutes in humidified CO_2 [5% (v/v) in air] at 37°C. Following BAPTA loading, Pb_1-lacking oocytes were either injected with sperm heads (ICSI) or challenged to activation by $SrCl_2$, ethanol or TPEN as described elsewhere. Meiotic progression was confirmed after 2 hours of continued incubation in KSOM in humidified CO_2 at 37°C by the presence of a Pb_2 with or without Tuba/DNA fluorescence imaging.

The membrane permeant AM ester forms of Zn^{2+}-sensitive dyes, FluoZin-3 (Invitrogen, CA, USA) or RhodZin-3 (Invitrogen), were used to measure relative ooplasmic [Zn^{2+}]$_c$. Oocytes were incubated in KSOM containing 10 μM FluoZin-3 or RhodZin-3 for 30 minutes either prior to, or following, ICSI or exposure to ethanol, $SrCl_2$ or TPEN. Fluorescence was monitored following excitation respectively at 470/40 nm (FluoZin-3) or 540/25 nm (RhodZin-3) and emission detection at 535/50 (FluoZin-3) or 605/55 nm (RhodZin-3) using a BioZero-8000 microscope/detector (Keyence, Osaka, Japan) and analyzed with BZ-Analyzer software (Keyence).

Protein fluorescence imaging

Immunocytochemistry, differential interference contrast microscopy (DIC) and epifluorescence imaging were essentially as described previously (Yoshida et al., 2007a). Cortical granule staining after sample fixation [4% (w/v) paraformaldehyde] was with 100 μg/ml fluorescein isothiocyanate (FITC)-conjugated lens culinaris agglutinin (Sigma). Images of live oocytes following cRNA injection were captured via a BZ-8000 (Keyence) and analyzed using BZ-Analyzer software (Keyence). Excitation at 540/25 nm was used with a TRITC (red) filter system for mCherry fluorescence detection and at 480/30 nm with a GFP (green) filter system to detect Venus epifluorescence.

The response of mII oocytes to TPEN was visualized by time-lapse microscopy of oocytes containing a Venus-tubulin-α (Tuba) fusion protein whose expression was driven by the *ZP3* transgene promoter on a C57BL/6×C3H background (subsequently back-crossed to C57BL/6). The 4.5 kbp *Bci*VI-*Mlu*I *pZP3→Venus-Tuba* transgene fragment was generated by inserting a 2019 bp *pZP3*-containing *Xho*I-*Kpn*I genomic DNA fragment upstream of a 710 bp *Bam*HI-*Bsr*GI *Venus* fragment linked to a 1633 bp *Bsr*GI-*Mlu*I fragment from *pEGFP-Tuba*, which encodes human tubulin-α (Clontech Laboratories, CA, USA). Oocytes were placed in a KSOM droplet under mineral oil on a glass-bottomed dish containing 100 μM TPEN on the stage of a TE2000 inverted microscope (Nikon, Japan) equipped with a CSU10 confocal scanning unit (Yokogawa, Japan) and a humidified chamber [5% (v/v) CO_2 in air] at 37°C. DIC images and fluorescent (488 nm) images (typically 13 focal planes, step size=2 μm) were captured at 5-minute intervals by a C9100-13 ImagEM EM-CCD camera (Hamamatsu Photonics, Shizuoka, Japan) driven by MetaMorph (Molecular Devices, CA, USA) image analysis software.

Sperm preparation, microinjection and nuclear transfer

Sperm preparations were as described previously, with minor modifications (Yoshida et al., 2007b). Briefly, cauda epididymidal spermatozoa from 12- to 30-week-old male $B6D2F_1$ mice were triturated in nuclear isolation medium [NIM: 125 mM KCl, 2.6 mM NaCl, 7.8 mM Na_2HPO_4, 1.4 mM KH_2PO_4, 3.0 mM EDTA (pH 7.45)] containing 1.0% (w/v) 3-[(3-cholamidopropyl)dimethylammonio]-1-propanesulfonate (CHAPS) at room temperature (25°C) for 1 minute. Sperm were washed twice in ambient temperature NIM to give control de-membranated heads, cHds. Where appropriate, sperm suspensions (or part thereof) were incubated at 48°C for 30 minutes, with trituration after 15 minutes, to generate 'inactivated', iHd preparations. (Sperm preparations contained all sperm-derived debris, including tails, mid-pieces and other fragments, but only heads were injected.) Sperm were mixed with one to two volumes of 15% (w/v) PVP_{360} (average M_r=360,000; Kanto Chemical, Tokyo, Japan) and microinjected as described (Yoshida and Perry, 2007), typically within 30 minutes of PVP mixing. Batches of oocytes were typically injected within 15 minutes and activation immediately induced by exposure to $SrCl_2$ (Perry et al., 2000), ethanol or TPEN followed by washing in KSOM and continuing KSOM incubation in 5% (v/v) CO_2 humidified air at 37°C. Parthenogenetic activation of iHd-injected oocytes was as described above, within 30 minutes of injection. Cumulus cell nuclear transfer into enucleated mII oocytes was essentially as described previously (Wakayama et al., 1998) with TPEN activation one to two hours post nuclear transfer, where appropriate.

PCR

Ratiometric quantification of mRNAs (qPCR) in day 4.5 (E4.5, 96 hours) embryos was essentially as described previously (Amanai et al., 2006; Shoji et al., 2006) using the following primer pairs (5′ to 3′): *H2afz*, GCGTATCACCCCTCGTCACTTG and TCTTCTGTTGTCCTTTCTTCCCG; *Pou5f1* (*Oct4*), CGTGAAGTTGGAGAAGGTGGAACC and GCAGCTTGGCAAACTGTTCTAGCTC; *Sox2*, GGAAAAAAACCACCAATCCCATCC and TTTGCGAACTCCCTGCGAAG; *Nanog*, GCAAGCGGTGGCAGAAAAAC and GCAATGGATGCTGGGATACTCC; *Cdx2*, GGAAGCCAAGTGAAAACCAG and CTTGGCTCTGCGGTTCTG; *Socs3*, GCAGATCAACAGATGAGCCA and TGGGACAGAGGGCATTTAAG; *Eif3s10*, AAGGGGTGATGATGCAAGAC and AGGTGGACCCCAACTCTCTT. Eight samples per group were analyzed in triplicate per primer pair and data normalized with respect to *H2afz*.

Immunological methods

Standard immunoblotting (IB) for Fig. 2B was with rabbit polyclonal anti-CycB1 [Santa Cruz Biotechnology, CA, USA; 1:500 (v/v)], anti-Tubg (γ-tubulin; Abcam, MA, USA; 1:100 (v/v)], rabbit monoclonal anti-phosphoErk1/2 [Cell Signaling Technology, MA, USA; 1:1000 (v/v)], rabbit polyclonal anti-Erk1/2 [Cell Signaling; 1:1000 (v/v)], or rabbit polyclonal anti-Tuba [α-tubulin; Abcam; 1:1000 (v/v)] primary antibodies, and anti-rabbit IgG [Invitrogen, CA, USA; 1:10,000 (v/v)] secondary antibody.

Blastocyst cell counting

E4.5 embryos were fixed [4% (w/v) paraformaldehyde] and subjected to standard incubation at 4°C overnight in rabbit anti-Oct4 (1:10,000; a kind gift from Dr H. Niwa) and for 1 hour at 37°C in mouse anti-Cdx2 (1:100; MU392-UC, BioGenex Laboratories, CA, USA), followed by a 1 hour incubation at 37°C in Alexa 488-conjugated anti-rabbit IgG (Invitrogen) and TRITC-conjugated anti-mouse IgG (Sigma). Cells exclusively stained with Alexa were scored as Oct4-positive pluriblasts, and those exclusively TRITC staining, as Cdx2-positive trophoblasts.

Statistical methods

Unless stated otherwise, Student's t-tests were respectively applied to comparative unpaired analyses of Ca^{2+}_i oscillation and developmental frequencies. Pearson's chi-squared (χ^2) tests were performed where indicated. Data for each experiment were collected on at least 2 days.

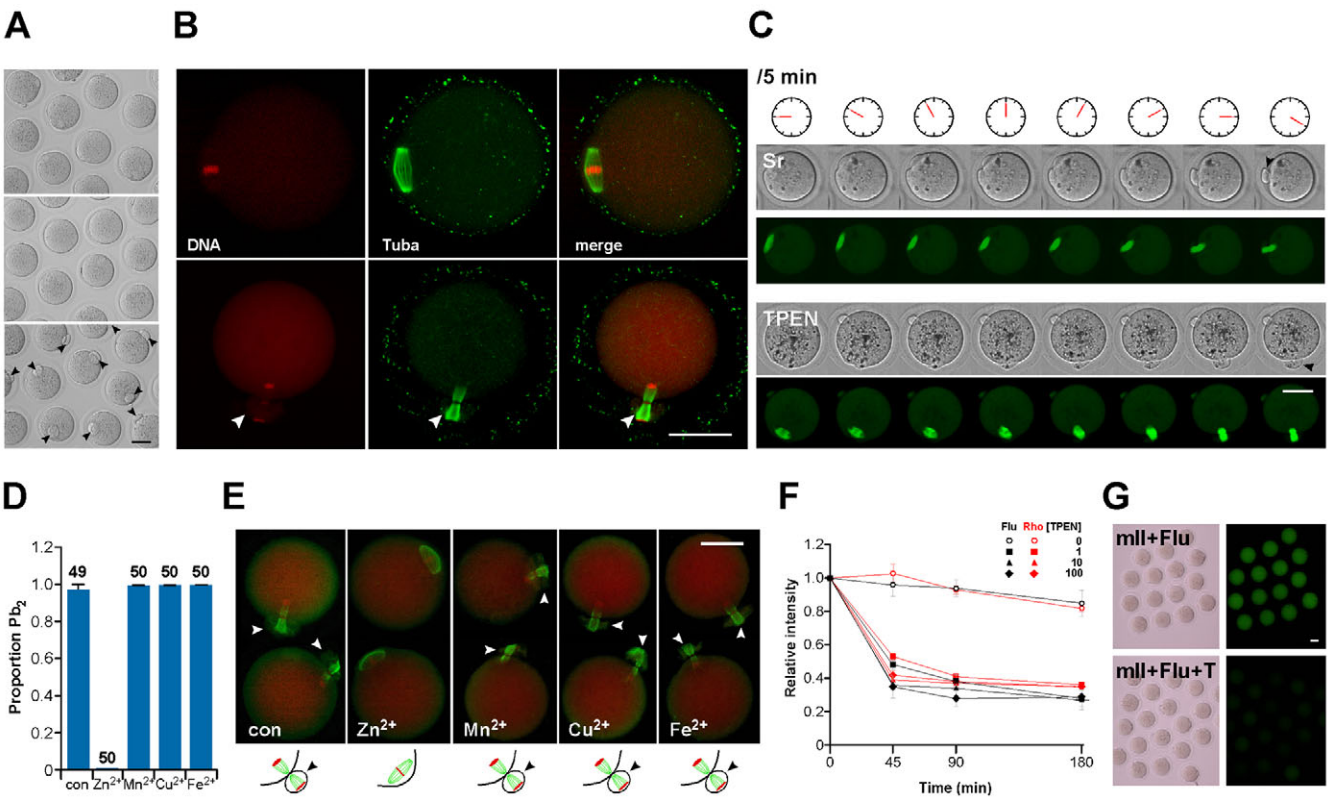

Fig. 1. Zn^{2+} Sequestration induces mII exit. (**A**) Hofmann images 1.5 hours after incubating mII oocytes in KSOM (top), DMSO alone (middle) or 100 μM TPEN (bottom). (**B**) Immunofluorescence microscopy of mII oocytes alone (top) or 1.5 hours after 100 μM TPEN treatment (bottom). Tubulin-α (Tuba) appears green and genomic DNA appears red. (**C**) Paired DIC (top) and Venus fluorescence images of Venus-Tuba-expressing oocytes (5-minute intervals) exposed to 10 mM $SrCl_2$ (Sr, upper panels) or 100 μM TPEN (lower panels). Sequences start ~45 minutes after initial exposure. (**D**) Second polar body (Pb_2) extrusion 1.5 hours after parallel incubation of mII oocytes with 100 μM TPEN (con) or 100 μM TPEN plus the cations indicated (100 μM) showing oocyte numbers. (**E**) Oocytes following sequential TPEN-cation incubation (see Fig. S1C in the supplementary material) stained as in B, with schematics. (**F**) Oocytes loaded with FluoZin-3 (black lines) or RhodZin-3 (red) and transferred at *t*=0 (fluorescence level=1.0) to KSOM containing 100 μM TPEN. (**G**) Paired Hofmann (left) and comparative epifluorescence (480 nm) (right) images of mII oocytes loaded with FluoZin-3 (Flu, top) and 1.5 hours after 100 μM TPEN treatment (bottom). Scale bars: 50 μm in A-C,E,G. Error bars indicate s.e.m. Arrowheads indicate the second polar body.

RESULTS

Zn^{2+} is required to maintain mII arrest in mouse oocytes

To determine whether Zn^{2+} played a role in mouse mII arrest, we exposed intact oocytes to the selective Zn^{2+} chelator, *N,N,N′,N′*-tetrakis-(2-pyridylmethyl)-ethylenediamine (TPEN), which exhibits a low affinity for Ca^{2+} ($k_{d[Ca]}$=4.0×10^{-5} M, $k_{d[Zn]}$=2.6×10^{-16} M) (Arslan et al., 1985). All underwent dose-dependent mII exit, evidenced by spindle movement and Pb_2 extrusion, with kinetics for 100 μM TPEN (100 μM is used throughout unless stated otherwise) similar to those of the parthenogenetic agent, $SrCl_2$ at 10 mM (80.6±1.3 and 73.4±1.4 minutes, respectively, *n*=25 and *n*=22) (Fig. 1A-C; see Fig. S1A in the supplementary material). Chelating agents selective for Mn^{2+}, Cu^{2+} or Fe^{2+} did not induce oocyte activation (see Fig. S1B in the supplementary material). Meiotic release by TPEN was inhibited by parallel or sequential incubation in 100 μM Zn^{2+} but not Mn^{2+}, Cu^{2+} or Fe^{2+} (Fig. 1D,E; see Fig. S1C in the supplementary material). To ascertain the effect of TPEN on levels of exchangeable cytoplasmic Zn^{2+} $(Zn^{2+})_c$, oocytes were loaded with the Zn^{2+}-sensitive fluorescent probes, FluoZin-3 or RhodZin-3. These have k_ds for Zn^{2+} at least seven orders of magnitude higher than that of TPEN (see Table S1 in the supplementary material) and did not induce mII exit. FluoZin-3 and RhodZin-3 fluorescence decreased in response to TPEN (Fig. 1F,G), correlating TPEN treatment, mII exit and $[Zn^{2+}]_c$. The TPEN-induced decrease in FluoZin-3 fluorescence was reversed by 100 μM Zn^{2+} (see Fig. S1D in the supplementary material). Exposure of FluoZin-3-loaded mII oocytes to Sr^{2+} (which induces mII exit) but not Mn^{2+} or Fe^{2+} (which do not) elicited a 50% decrease in fluorescence within 15 minutes (see Fig. S2 in the supplementary material), but induction of mII exit by intracytoplasmic sperm injection (ICSI) did not induce analogous $Zn^{2+}{}_c$ redistribution.

Meiotic exit Induced by Zn^{2+} depletion neither requires nor mobilizes $Ca^{2+}{}_i$

The mobilization of $Ca^{2+}{}_i$ is ubiquitous in fertilization (Stricker, 1999). Sequestration of $Ca^{2+}{}_i$ with BAPTA (Kline and Kline, 1992) prevented the induction of mII exit (Pb_2 extrusion) by sperm, ethanol or $SrCl_2$, but had no effect on TPEN-induced meiotic progression (Fig. 2A,B). Exposure of oocytes to TPEN did not induce a $[Ca^{2+}{}_i]$ increase (0/37), unlike sperm (*n*=26) or $SrCl_2$ (*n*=15) (Fig. 2C; see Fig. S3A in the supplementary material). TPEN was washed out after treatment and $[Ca^{2+}{}_i]$ recording was initiated within ~30-120 seconds, but no $[Ca^{2+}{}_i]$ change was observed (*n*=40) over 6 hours.

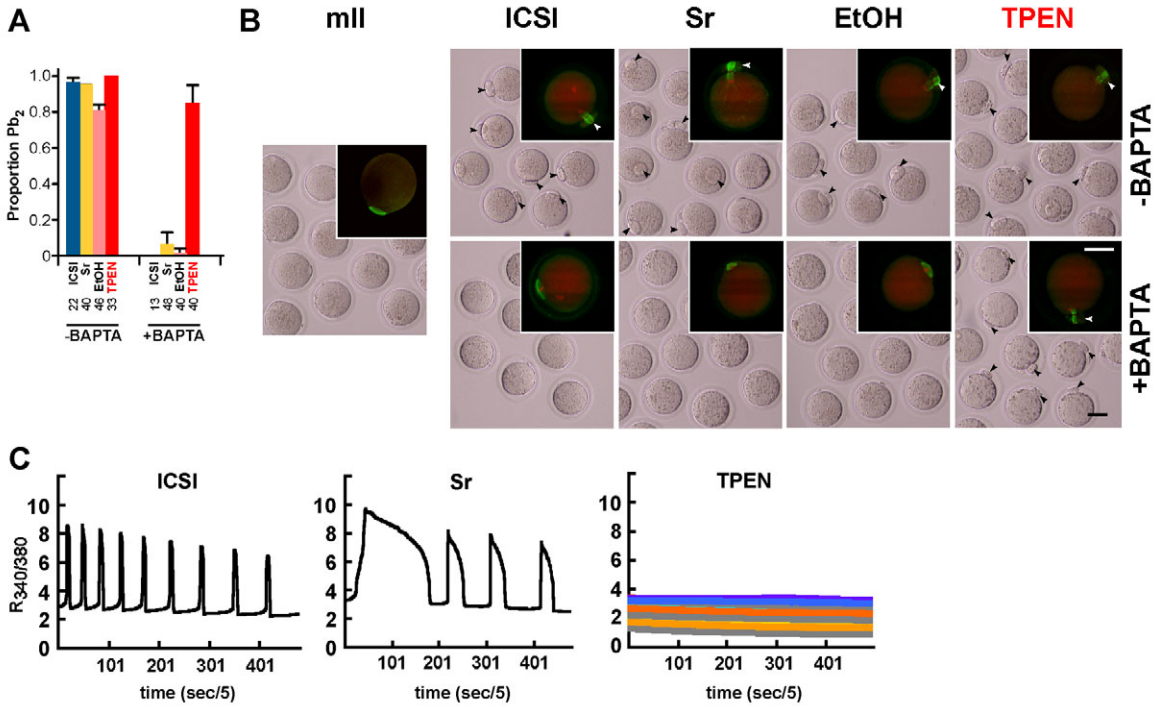

Fig. 2. TPEN-induced meiotic exit is Ca^{2+}_i independent and does not cause Ca^{2+}_i release. (**A**) Proportion of oocytes undergoing mII exit (Pb_2 extrusion) after incubation for 20 minutes in KSOM with (+BAPTA) or without 50 μM BAPTA prior to ICSI or to exposure to 10 mM $SrCl_2$ (Sr), 7% (v/v) ethanol (EtOH) or 100 μM TPEN as indicated. Numbers of oocytes/group are shown. Error bars indicate s.e.m. (**B**) Hofmann images of representative oocytes in A, showing fluorescence (insets) micrographs for Tuba (green) and DNA (red). Arrowheads indicate Pb_2. Error bars indicate s.e.m. (**C**) Ratiometric fura-2 [Ca^{2+}_i] imaging (5-second intervals) of representative mII oocytes following sperm head injection (ICSI), or continued exposure to 10 mM $SrCl_2$ (Sr) or 100 μM TPEN; the panel representing TPEN treatment shows 22 traces.

TPEN also inhibited Ca^{2+}_i mobilization, as pre-incubation with TPEN prevented [Ca^{2+}_i] oscillations in response to Sr^{2+} and reduced the frequencies of both ICSI- and inositol 1,4,5-trisphosphate-induced [Ca^{2+}_i] oscillations (see Fig. S3B,C in the supplementary material) (Lawrence et al., 1998). The reduction of ICSI-induced oscillations was significantly (P<0.0001) rescued by 100 μM Zn^{2+}, although Zn^{2+} had no effect on ICSI-induced oscillations per se (see Fig. S3C in the supplementary material). These findings indicate potent inhibition of IP_3 signaling and Ca^{2+} release by TPEN and that Zn^{2+} depletion induces meiotic exit independently of Ca^{2+}_i.

TPEN delineates Ca^{2+}_i-dependent oocyte activation events

Mammalian fertilization induces oocyte APC activation, degradation of proteasomal targets, including Emi2 and CycB, and cortical granule (CG) exocytosis (a vesicle fusion event) (Runft et al., 2002; Schmidt et al., 2005; Madgwick et al., 2006; Perry and Verlhac, 2008). We investigated whether TPEN also induced these events, first estimating changes in relative Emi2 levels. When mII oocytes were injected with complementary RNA (cRNA) encoding Emi2-mCherry and challenged 4 hours later with either sperm or $SrCl_2$, Emi2 degradation was rapid; sperm induced a 50% fluorescence decline in 14.1 minutes (Fig. 3A). TPEN treatment did not effect Emi2-mCherry levels (Fig. 3A) but induced depletion of endogenous phospho-MAPK and CycB1 (Fig. 3B), and CycB1-Venus (in oocytes injected with CycB1-Venus cRNA; Fig. 3C), with similar kinetics to those induced by sperm or $SrCl_2$. To determine whether Emi2 degradation required Zn^{2+}_c, oocytes expressing Emi2-mCherry were pre-incubated with TPEN and then exposed to ethanol. Controls treated with ethanol alone (n=36) all underwent [Ca^{2+}_i] release and marked loss of Emi2-mCherry fluorescence, although most oocytes treated with TPEN and then ethanol (30/38) underwent a Ca^{2+}_i rise without Emi2-mCherry degradation (Fig. 3D; not shown). This suggests that a Ca^{2+} signal is insufficient to ensure Emi2 degradation in the absence of Zn^{2+}_c.

TPEN-induced mII exit and recombinant CycB1 degradation were prevented by the 26S proteasome inhibitors epoxomicin or Z-LLL-CHO (Fig. 3E,F). When the APC activator Cdc20 was reduced to less than 10% of control levels by RNAi (Shoji et al., 2006; Amanai et al., 2006), TPEN treatment failed to induce mII exit (Fig. 3G). Mouse mII exit requires an intact spindle (Kubiak et al., 1993). Consistent with this, microtubule disruption by nocodazole completely prevented activation by either $SrCl_2$ (n=16) or TPEN (n=27). TPEN treatment also failed to induce CG exocytosis (Fig. 3H). Thus, Zn^{2+} chelation destabilizes mII arrest in a Cdc20- and microtubule-dependent, but Ca^{2+}_i-independent, manner that requires proteasomal activity.

Developmental consequences of oocyte Zn^{2+} sequestration

The finding that TPEN induces [Ca^{2+}_i]-static meiotic resumption raised the issue of whether resultant embryos could develop and caused us to examine the developmental role of fertilization-induced [Ca^{2+}_i] changes. Oocytes activated by continual TPEN exposure rarely developed beyond two cells, suggesting embryotoxicity. Those exposed for only 45 minutes (in the presence of the microfilament inhibitor, cytochalasin B, to prevent cytokinesis and therefore loss of maternal chromosomes) produced

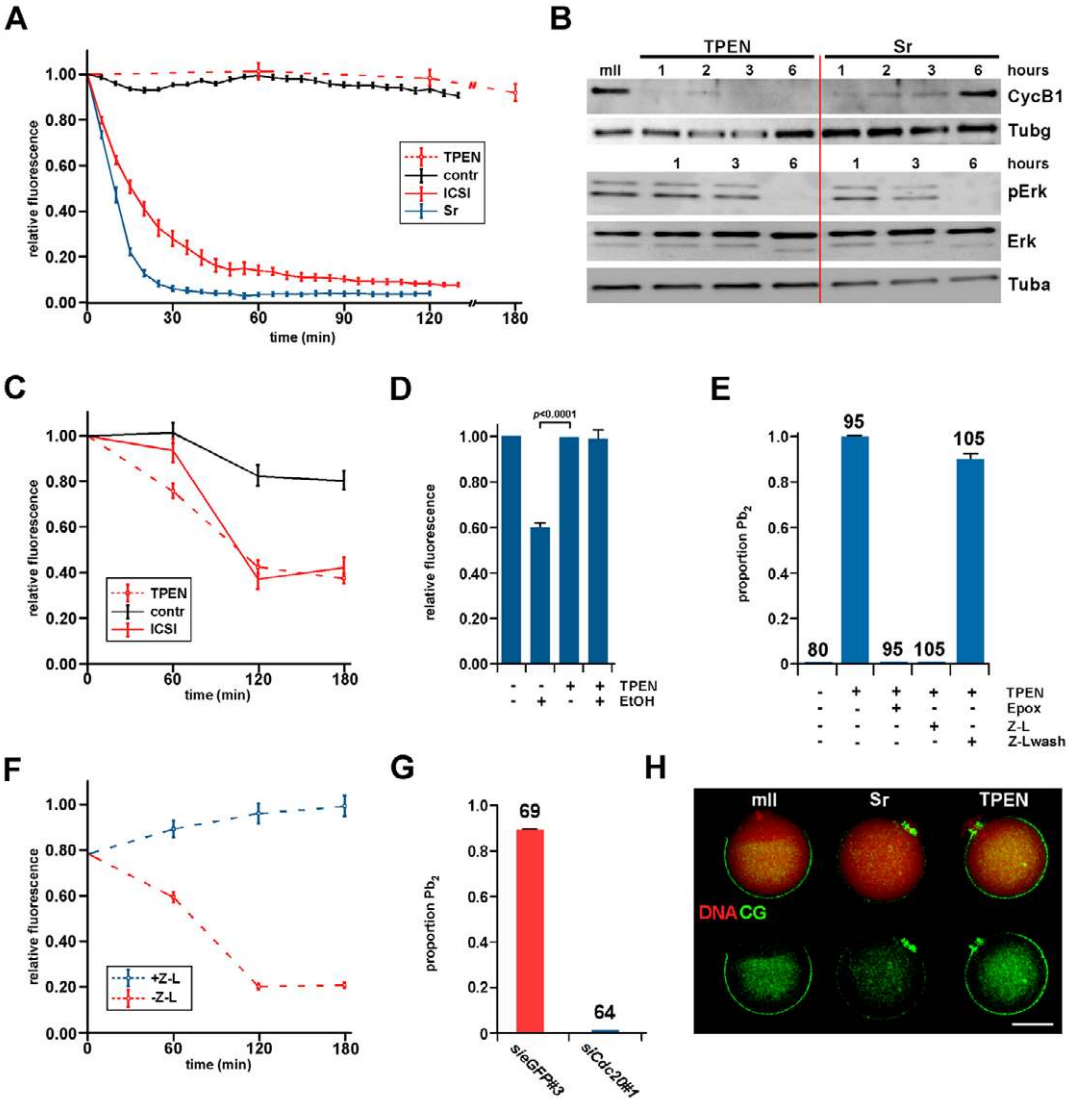

Fig. 3. Zn^{2+}_i sequestration induces proteasome-dependent mII exit but not Emi2 degradation or cortical granule exocytosis. (**A**) Relative mCherry fluorescence intensities in oocytes injected with cRNA encoding Emi2-mCherry, followed 4 hours later (at *t*=0) by continued incubation alone (contr) or by a sperm injection challenge (ICSI), treatment with10 mM $SrCl_2$ (Sr) or treatment with 100 μM TPEN (TPEN). Recording was initiated at *t*=0. (**B**) Immunoblots of control mII oocytes (mII) and, at the times shown (hours), oocytes activated with 100 μM TPEN or 10 mM $SrCl_2$ (Sr), probed for endogenous CycB1 (100 oocytes/track) or active phospho-Erk (pErk, 70 oocytes/track), then reprobed with a pan-Erk antibody. Tuba and Tubg indicate loading equivalence. (**C**) As for A, but recording Venus fluorescence following injection of cRNA encoding CycB1-Venus. (**D**) Relative mCherry fluorescence in oocytes injected with cRNA encoding Emi2-mCherry and then (after 4 hours) exposed to TPEN and/or ethanol (EtOH) for 1 hour. (**E**) Proportion of mII oocytes undergoing Pb_2 extrusion after 1.5 hours exposure to 100 μM TPEN, epoxomicin (Epox), Z-LLL-CHO (Z-L) or Z-LLL-CHO, followed by washing and 3 hours further culture in KSOM alone (Z-Lwash). (**F**) Relative fluorescence in mII oocytes injected with cRNA encoding CycB1-Venus then incubated (4 hours later, *t*=0) in 100 μM TPEN in the presence (+Z-L) or absence of Z-LLL-CHO. (**G**) Injection of mII oocytes with *sieGFP* or *siCdc20* siRNA followed 7 hours later by treatment with 100 μM TPEN, showing the proportion of oocytes undergoing Pb_2 extrusion 1.5 hours after treatment. (**H**) Untreated oocytes (mII) or oocytes exposed for 2 hours to either 10 mM $SrCl_2$ (Sr) or 100 μM TPEN. FITC-labeled cortical granules (green) and DNA (red) are shown. Scale bar: 50 μm. Error bars indicate s.e.m.

27.3±13.7% diploid parthenogenetic blastocysts (Fig. 4A) and when supplemented with 100 μM $ZnSO_4$ for 3 hours post-TPEN, expanded blastocyst development improved to 75.3±3.7% by embryonic day 4.5 (E4.5, 96 hours) (Fig. 4A,B). The transition metal cations Mn^{2+}, Cu^{2+}, Fe^{2+}, Ni^{2+} or Co^{2+} did not rescue TPEN toxicity (Fig. 4C), indicating that embryotoxicity had been specifically due to Zn^{2+} deprivation. We also applied the TPEN activation regimen to cumulus cell nuclear transfer (Fig. 4D). Development in vitro to the expanded blastocyst stage at E4.5 following the transfer of cumulus cell nuclei and activation with $SrCl_2$ (19.6% of pronuclear zygotes) was markedly reduced when activation was with TPEN (7.6%, $P<0.0001$) (Fig. 4D). Activation with $SrCl_2$ followed by treatment with TPEN also resulted in low developmental rates of nuclear transfer embryos (1.7%; Fig. 4D).

Diploid E4.5 parthenogenotes arising from TPEN or $SrCl_2$ activation contained similar levels of *Oct4* (*Pou5f1*), *Sox2*, *Nanog* and *Cdx2* (Fig. 4E), although the TPEN group had fewer Oct4- and

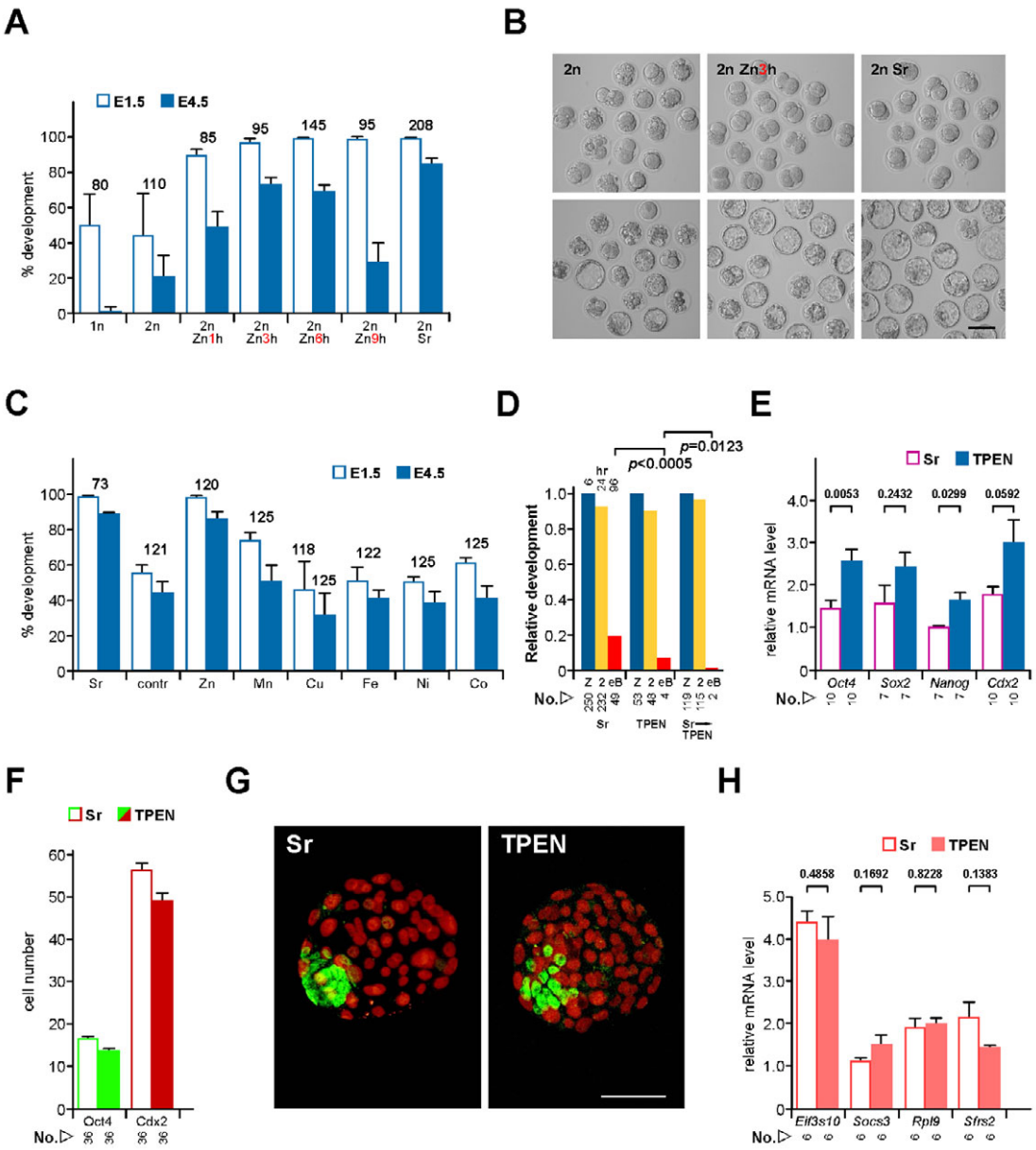

Fig. 4. Embryo development in vitro following TPEN-induced meiotic exit. (**A**) Development to the two-cell (open) or blastocyst stages at E1.5 (E1.5) or E4.5, respectively, initiated by exposure of mII oocytes to 100 μM TPEN for 45 minutes in the absence (1n) or presence (2n) of cytochalasin B, followed by exposure to 100 μM $ZnSO_4$ (Zn) for 1, 3, 6 or 9 hours, as indicated. 2n Sr indicates activation by 10 mM $SrCl_2$ in the presence of cytochalasin B. Values above columns indicate embryo numbers/group. (**B**) Representative embryos from A at E1.5 (upper) and E4.5; the key is as for A. Scale bar: 100 μm. (**C**) Development to the two-cell (open) or blastocyst stages at E1.5 and E4.5, respectively, initiated by exposure of mII oocytes to 100 μM TPEN for 45 minutes in the presence of cytochalasin B, followed by incubation in KSOM without a supplement (con) or supplemented for 3 hours with 100 μM Zn^{2+} (Zn), Mn^{2+} (Mn), Fe^{2+} (Fe), Cu^{2+} (Cu), Ni^{2+} (Ni) or Co^{2+} (Co). Values above columns indicate embryo numbers/group. (**D**) Development relative to pseudopronuclear zygotes (=1.0) of cumulus cell nuclear transfer two-cell embryos (2C, 24 hours), and expanded blastocysts (eB, 96 hours) generated by exposure to 10 mM $SrCl_2$ (Sr), to TPEN or to $SrCl_2$ followed by TPEN. (**E**) Ratiometric PCR (qPCR) for the transcripts indicated in embryos 96 hours after activation (E4.5). Sr, activation by 10 mM $SrCl_2$ in the presence of cytochalasin B (without TPEN) and subsequent incubation in KSOM. Cell counts (**F**) and fluorescence images (**G**) of cells stained for Oct4 (green) or Cdx2 (red) in E4.5 diploid embryos generated by activation with $SrCl_2$ (Sr) (open bars in F) or 100 μM TPEN. Scale bar in F: 50 μm. (**H**) qPCR as per E but for different (Ca^{2+}-sensitive) transcripts and embryos 60 hours post-activation (E2.5). Pearson's χ^2 values (p) are shown above columns in E and H. Numbers per group (n) are given beneath histograms in D-F,H. Error bars indicate s.e.m.

Cdx2-expressing cells (Fig. 4F,G). Transcripts whose levels are reportedly sensitive to $[Ca^{2+}_i]$ oscillations (Ozil et al., 2006; Rogers et al., 2006), including *Eif3s10*, *Socs3*, *Rpl9* and *Sfrs2*, were present at similar levels in TPEN and $SrCl_2$ groups at E2.5 (Fig. 4H).

The sperm-borne signal for the $[Ca^{2+}_i]$ rise can be inactivated by heating, so that sperm heads ('inactivated heads', iHds) do not elicit mII exit (Fig. 5A) (Perry et al., 1999; Perry et al., 2000; Yoshida et al., 2007b). Exposure of iHd-injected oocytes to $SrCl_2$

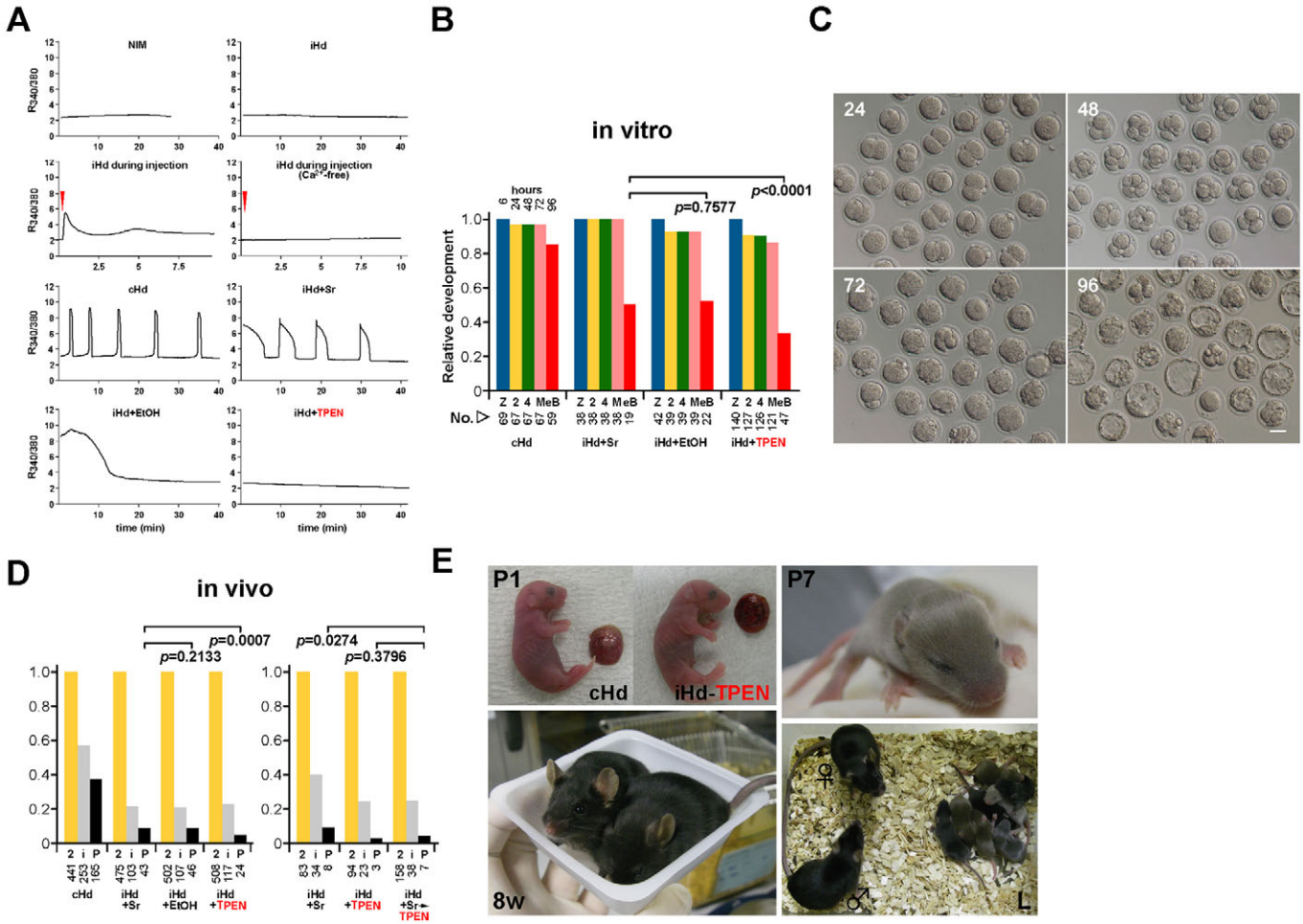

Fig. 5. Full-term development after TPEN-induced mII exit without $Ca^{2+}{}_i$ mobilization. (**A**) Ratiometric fura-2 $Ca^{2+}{}_i$ imaging (5-second intervals) of representative oocytes following control (cHd) or 'inactivated' sperm head (iHd) injection alone, or iHd injection followed by exposure to activating agents 10 mM $SrCl_2$ (iHd+Sr), 7% ethanol (iHd+EtOH) or 100 μM TPEN (iHd+TPEN). Red arrowheads indicate the moment of iHd injection, while readings were in progress. (**B**) Development in vitro of oocytes injected with cHd or with iHd followed by exposure to activating agents shown to two-cell (2), four-cell (4), morula (M) and expanded blastocyst (eB) stages relative to pronuclear zygotes (Z, 1.0). (**C**) Representative embryos from B after TPEN-induced activation at the times shown (hours). (**D**) Development in vivo following injection of oocytes with cHd or iHd as in B, relative to two-cell embryos transferred, showing implantation fossae (i) and pups (P), with absolute values (No.). *p* values, χ^2. (**E**) TPEN-derived offspring from D: at term (P1, also showing cHd control); on postnatal day 7 (7); at 8 weeks (8w). A male and female with their healthy litter (L) is also shown.

or ethanol, respectively, induced [$Ca^{2+}{}_i$] oscillations or a prolonged monotonic [$Ca^{2+}{}_i$] rise (Rickords and White, 1993), whereas 194/195 (99.49%) exposed to TPEN exhibited no [$Ca^{2+}{}_i$] change (Fig. 5A), with one case undergoing a single small bell-shaped release lasting 3.16 minutes, which was insufficient to induce mII exit (Kline and Kline, 1992). Embryos in $SrCl_2$ and ethanol groups developed comparably in vitro with good, if poorer, development in the TPEN group (Fig. 5B,C). Following two-cell embryo transfer, $SrCl_2$ and ethanol groups yielded equivalent full-term development (respectively, 9.0 and 9.2% of transfers; P=0.758); TPEN-induced development produced 24 offspring (4.7%) that grew into healthy fertile adults (Fig. 5D,E). This lower rate probably reflects TPEN embryotoxicity rather than lack of [$Ca^{2+}{}_i$] mobilization, as iHd-injected oocyte exposure to TPEN, or to $SrCl_2$ (i.e. activation with [$Ca^{2+}{}_i$] oscillations) followed by TPEN, yielded similar rates (P=0.380) of full-term development (Fig. 5D). Recording $Ca^{2+}{}_i$ levels during iHd injection in standard medium showed a small transient rise (n=4), but no rise in Ca^{2+}-free medium (n=4; Fig. 5A). TPEN activation of oocytes injected with iHds in Ca^{2+}-free medium (eliminating external Ca^{2+} influx during injection; Fig. 5A) caused pronounced oocyte trauma that frequently resulted in death, yet we obtained three offspring from 175 embryos (1.7%). Full-term development is therefore not conditioned upon $Ca^{2+}{}_i$ release during mII exit and [$Ca^{2+}{}_i$] oscillations do not assure an altered rate of full-term development compared with a single [$Ca^{2+}{}_i$] rise.

DISCUSSION

This work delineates roles of Zn^{2+} and Ca^{2+} during mammalian mII and mII exit. From the results obtained, it can be argued that Zn^{2+} is required for mII arrest and that $Ca^{2+}{}_i$ release during fertilization is not essential for full-term development. The work provides evidence that Zn^{2+} is required for the Emi2-mediated

regulation of meiotic arrest in mouse mII oocytes. Meiotic resumption after Zn^{2+} depletion is not accompanied either by Ca^{2+} release or Emi2 degradation, both of which are induced by Ca^{2+}-dependent oocyte activation (Fig. 2A-C; Fig. 3A). Furthermore, events of mII exit that depend on the APC-proteasome pathway, including cyclin B degradation and chromosome separation (Peters, 2006), occur with similar kinetics whether or not Ca^{2+} is mobilized (Fig. 1A-C; Fig. 3B,C). This observation implies that Zn^{2+} depletion activates or unmasks the APC-proteasome pathway, even in the presence of Emi2. Indeed, TPEN-induced mII exit is prevented by proteasome inhibitors (Fig. 3E,F) or removal of the APC activator Cdc20 by RNAi (Fig. 3G). Finally, Emi2 contains a putative zinc-binding region and, unlike Emi2, other cytostatic factor candidates have been shown to be dispensable for mouse mII arrest, including Emi1, Mos (Shoji et al., 2006) and spindle assembly checkpoint proteins Bub1, Mad2 and BubR1 (Tsurumi et al., 2004).

Induction of mII exit by sperm, $SrCl_2$ or ethanol – but not TPEN – is accompanied by Emi2 disappearance (Fig. 3A), suggesting that Emi2 degradation requires Ca^{2+} release. As Emi1 undergoes SCF^{Trcpb}-mediated destruction in response to phosphorylation by Plk1 (Hansen et al., 2004), this requirement could be due to Ca^{2+}-dependent kinases that become activated during fertilization and phosphorylate Emi2 to target it for proteolysis. Sequential phosphorylation by CaMKII and Plk1 mediates the Ca^{2+}-sensitive degradation of *Xenopus* Emi2 (Rauh et al., 2005; Schmidt et al., 2005). Recent work employing RNAi or gene targeting suggests that CaMKIIγ plays an important role in physiological mII exit in the mouse (Chang et al., 2009; Backs et al., 2010). However, it remains to be seen whether Emi2 degradation is CaMKIIγ-dependent as it is in *Xenopus* (Rauh et al., 2005). Our result that depletion of Zn^{2+} inhibits ethanol-induced Emi2 degradation (Fig. 3D) implies that Zn^{2+} might also be involved in Emi2 degradation during mII exit. It remains to be seen precisely how mouse Emi2 degradation is controlled at meiotic resumption and why Emi1 and Emi2 – unlike Mad2 – have evolved a Zn^{2+}-dependent mechanism for APC inhibition (Reimann et al., 2001b; Herzog et al., 2009).

Emi2 depletion induces meiotic exit (Shoji et al., 2006) and its degradation is caused by Ca^{2+}_i release. Our results show that neither Ca^{2+}_i release nor Emi2 degradation at the time of mII exit is essential for full-term development. It may be inferred that Emi2 destruction is the sole indispensable role of Ca^{2+} release during meiotic exit. We did not observe Ca^{2+} release at any time before, during or after the addition of TPEN to, or release of TPEN from, oocytes in procedures that produced offspring, including iHd injection in Ca^{2+}-free medium (Fig. 5A). It has previously been reported that the characteristics of Ca^{2+} signaling at fertilization are important for multiple events of oocyte activation and later development in vitro (Ducibella et al., 2002; Ozil et al., 2005; Rogers et al., 2006) and in vivo (Ozil et al., 2006). These studies modulated Ca^{2+}_i dynamics in Ca^{2+}-free media, or with electropermeabilization or the eukaryotic protein synthesis inhibitor cycloheximide. Electrical pulses and protracted Ca^{2+} deprivation may influence development owing to variables other than Ca^{2+}_i mobilization, reflecting limited specificity or secondary effects. The negative developmental effects of cycloheximide (Rogers et al., 2006) were rescued by co-incubation with ethanol or Sr^{2+}, but only when the co-incubation followed relatively brief cycloheximide exposure – too little for any demonstrable effect – and without allowing for the possibility that Ca^{2+} or Sr^{2+} treatment is antagonistic to cycloheximide activity.

When mII exit was induced by oscillations (Sr^{2+}) or a monotonic Ca^{2+} rise (ethanol) just after iHd injection, embryos developed at indistinguishable rates, arguing against developmental enhancement by Ca^{2+} oscillations. Given the clear implication that Ca^{2+}_i oscillations are dispensable during mouse fertilization, the issue arises as to their function. The regulation of APC^{Cdc20} by Emi2 to sustain mII arrest and the precipitous degradation of Emi2 following activation (Fig. 3A) argue against cumulative CycB degradation with each Ca^{2+}_i oscillation (Shoji et al., 2006; Ducibella and Fissore, 2008). Rather, it is possible that the main function of oscillations is as a fail-safe to peg the $[Ca^{2+}_i]$ to sub-cytotoxic levels while periodically enabling Ca^{2+} signaling; enduringly elevated $[Ca^{2+}_i]$ causes oocyte death and persistence until pronucleus formation may ensure that [Emi2] remains low until Emi2 mRNA levels decline (Berridge, 1987; Perry et al., 1999; Perry et al., 2000; Fujimoto et al., 2004).

This is perhaps the first definitive role for Zn^{2+} in the oocyte, but it is unlikely to be the last given the range of biological functions that Zn^{2+} controls and the subtle regulatory complexity of the oocyte-to-embryo transition. Development of embryos is poor following Zn^{2+} sequestration (relative to non-sequestration), even when accompanied by Ca^{2+} release (Fig. 5D). Potential physiological roles for Zn^{2+} in ensuring the gamete-to-embryo transition include transcription, signaling, histone modification and chromatin remodeling (Yamasaki et al., 2007; Bottomley et al., 2008; Maret, 2009; Viiri et al., 2009). These roles could account for the observation that nuclear transfer TPEN embryos arrest at the two-cell stage (Fig. 4D). Two-cell arrest also occurs in embryos lacking Brg1, which binds to zinc-finger proteins through a unique N-terminal domain and is essential in mice for the general activation of zygotic transcription and oocyte-to-zygote transition (Kadam and Emerson, 2003; Bultman et al., 2006). Although Brg1 is not known to bind Zn^{2+}, disruption of Zn^{2+} homeostasis could perturb the Brg1 regulatory network and others involving Zn^{2+}. We cannot exclude the possibility that technical aspects of Zn^{2+} depletion and nuclear transfer have a synergistically negative effect, but development was initially normal and this is a topic of ongoing investigation. Manipulating oocyte $[Zn^{2+}]$ promises to pave the way for new approaches to understanding mechanisms that underlie early embryogenesis in mammals.

Acknowledgements
The authors are grateful to Drs Maki Asami, Christoph Klein, Karen Lee and Matthew VerMilyea for their constructive criticisms, and to LARGE for embryo transfers. This work was funded by RIKEN.

Competing interests statement
The authors declare no competing financial interests.

Supplementary material
Supplementary material for this article is available at
http://dev.biologists.org/lookup/suppl/doi:10.1242/dev.049791/-/DC1

References
Amanai, M., Shoji, S., Yoshida, N., Brahmajosyula, M. and Perry, A. C. F. (2006). Injection of mammalian metaphase II oocytes with short interfering RNAs to dissect meiotic and early mitotic events. *Biol. Reprod.* **75**, 891-898.
Arslan, P., Di Virgilio, F., Beltrame, M., Tsien, R. Y. and Pozzan, T. (1985). Cytosolic Ca^{2+} homeostasis in Ehrlich and Yoshida carcinomas. A new, membrane-permeant chelator of heavy metals reveals that these ascites tumor cell lines have normal cytosolic free Ca^{2+}. *J. Biol. Chem.* **260**, 2719-2727.
Backs, J., Stein, P., Backs, T., Duncan, F. E., Grueter, C. E., McAnally, J., Qi, X., Schultz, R. M. and Olson, E. N. (2010). The gamma isoform of CaM kinase II controls mouse egg activation by regulating cell cycle resumption. *Proc. Natl. Acad. Sci. USA* **107**, 81-86.

Berridge, M. J. (1987). Elementary and global aspects of calcium signalling. *J. Exp. Biol.* **200**, 315-319.
Bottomley, M. J., Lo Surdo, P., Di Giovine, P., Cirillo, A., Scarpelli, R., Ferrigno, F., Jones, P., Neddermann, P., De Francesco, R., Steinkühler, C. et al. (2008). Structural and functional analysis of the human HDAC4 catalytic domain reveals a regulatory structural zinc-binding domain. *J. Biol. Chem.* **283**, 26694-26704.
Bultman, S. J., Gebuhr, T. C., Pan, H., Svoboda, P., Schultz, R. M. and Magnuson, T. (2006). Maternal BRG1 regulates zygotic genome activation in the mouse. *Genes Dev.* **20**, 1744-1754.
Chang, H. Y., Minahan, K., Merriman, J. A. and Jones, K. T. (2009). Calmodulin-dependent protein kinase gamma 3 (CamKIIγ3) mediates the cell cycle resumption of metaphase II eggs in mouse. *Development* **136**, 4077-4081.
Chatot, C. L., Ziomek, C. A., Bavister, B. D., Lewis, J. L. and Torres, I. (1989). An improved culture medium supports development of random-bred 1-cell mouse embryos in vitro. *J. Reprod. Fertil.* **86**, 679-688.
Cuthbertson, K. S. and Cobbold, P. H. (1985). Phorbol ester and sperm activate mouse oocytes by inducing sustained oscillations in cell Ca^{2+}. *Nature* **316**, 541-542.
Ducibella, T. and Fissore, R. (2008). The roles of Ca^{2+}, downstream protein kinases, and oscillatory signaling in regulating fertilization and the activation of development. *Dev. Biol.* **315**, 257-279.
Ducibella, T., Huneau, D., Angelichio, E., Xu, Z., Schultz, R. M., Kopf, G. S., Fissore, R., Madoux, S. and Ozil, J. P. (2002). Egg-to-embryo transition is driven by differential responses to Ca^{2+} oscillation number. *Dev. Biol.* **250**, 280-291.
Fujimoto, S., Yoshida, N., Fukui, T., Amanai, M., Isobe, T., Itagaki, C., Izumi, T. and Perry, A. C. F. (2004). Mammalian phospholipase Cζ induces oocyte activation from the sperm perinuclear matrix. *Dev. Biol.* **274**, 370-383.
Gautier, J., Minshull, J., Lohka, M., Glotzer, M., Hunt, T. and Maller, J. L. (1990). Cyclin is a component of maturation-promoting factor from *Xenopus*. *Cell* **60**, 487-494.
Hansen, D. V., Loktev, A. V., Ban, K. H. and Jackson, P. K. (2004). Plk1 regulates activation of the anaphase promoting complex by phosphorylating and triggering $SCF^{\beta TrCP}$-dependent destruction of the APC Inhibitor Emi1. *Mol. Biol. Cell* **15**, 5623-5634.
Herzog, F., Primorac, I., Dube, P., Lenart, P., Sander, B., Mechtler, K., Stark, H. and Peters, J. M. (2009). Structure of the anaphase-promoting complex/cyclosome interacting with a mitotic checkpoint complex. *Science* **323**, 1477-1481.
Igusa, Y., Miyazaki, S. and Yamashita, N. (1983). Periodic hyperpolarizing responses in hamster and mouse eggs fertilized with mouse sperm. *J. Physiol.* **340**, 633-647.
Kadam, S. and Emerson, B. M. (2003). Transcriptional specificity of human SWI/SNF BRG1 and BRM chromatin remodeling complexes. *Mol. Cell* **11**, 377-389.
Kline, D. and Nuccitelli, R. (1985). The wave of activation current in the *Xenopus* egg. *Dev. Biol.* **111**, 471-487.
Kline, D. and Kline, J. T. (1992). Repetitive calcium transients and the role of calcium in exocytosis and cell cycle activation in the mouse egg. *Dev. Biol.* **149**, 80-89.
Knott, J. G., Gardner, A. J., Madgwick, S., Jones, K. T., Williams, C. J. and Schultz, R. M. (2006). Calmodulin-dependent protein kinase II triggers mouse egg activation and embryo development in the absence of Ca^{2+} oscillations. *Dev. Biol.* **296**, 388-395.
Kubiak, J. Z., Weber, M., de Pennart, H., Winston, N. J. and Maro, B. (1993). The metaphase II arrest in mouse oocytes is controlled through microtubule-dependent destruction of cyclin B in the presence of CSF. *EMBO J.* **12**, 3773-3778.
Lawrence, Y., Ozil, J. P. and Swann, K. (1998). The effects of a Ca^{2+} chelator and heavy-metal-ion chelators upon Ca^{2+} oscillations and activation at fertilization in mouse eggs suggest a role for repetitive Ca^{2+} increases. *Biochem. J.* **335**, 335-342.
Lorca, T., Cruzalegui, F. H., Fesquet, D., Cavadore, J. C., Mery, J., Means, A. and Dorée, M. (1993). Calmodulin-dependent protein kinase II mediates inactivation of MPF and CSF upon fertilization of *Xenopus* eggs. *Nature* **366**, 270-273.
Madgwick, S., Hansen, D. V., Levasseur, M., Jackson, P. K. and Jones, K. T. (2006). Mouse Emi2 is required to enter meiosis II by reestablishing cyclin B1 during interkinesis. *J. Cell Biol.* **174**, 791-801.
Maret, W. (2009). Molecular aspects of human cellular zinc homeostasis: redox control of zinc potentials and zinc signals. *Biometals* **22**, 149-157.
Markoulaki, S., Matson, S. and Ducibella, T. (2004). Fertilization stimulates long-lasting oscillations of CaMKII activity in mouse eggs. *Dev. Biol.* **272**, 15-25.
Mazia, D. (1937). The release of calcium in *Arbacia* eggs upon fertilization. *J. Cell. Comp. Physiol.* **10**, 291-304.
Miller, J. J., Summers, M. K., Hansen, D. V., Nachury, M. V., Lehman, N. L., Loktev, A. and Jackson, P. K. (2006). Emi1 stably binds and inhibits the anaphase-promoting complex/cyclosome as a pseudosubstrate inhibitor. *Genes Dev.* **20**, 2410-2420.
Miyazaki, S., Yuzaki, M., Nakada, K., Shirakawa, H., Nakanishi, S., Nakade, S. and Mikoshiba, K. (1992). Block of Ca^{2+} wave and Ca^{2+} oscillation by antibody to the inositol 1,4,5-trisphosphate receptor in fertilized hamster eggs. *Science* **257**, 251-255.
Mochida, S. and Hunt, T. (2007). Calcineurin is required to release *Xenopus* egg extracts from meiotic M phase. *Nature* **449**, 336-340.
Nishiyama, T., Yoshizaki, N., Kishimoto, T. and Ohsumi, K. (2007). Transient activation of calcineurin is essential to initiate embryonic development in *Xenopus laevis*. *Nature* **449**, 341-345.
Ozil, J. P., Markoulaki, S., Toth, S., Matson, S., Banrezes, B., Knott, J. G., Schultz, R. M., Huneau, D. and Ducibella, T. (2005). Egg activation events are regulated by the duration of a sustained $[Ca^{2+}]_{cyt}$ signal in the mouse. *Dev. Biol.* **282**, 39-54.
Ozil, J. P., Banrezes, B., Tóth, S., Pan, H. and Schultz, R. M. (2006). Ca^{2+} oscillatory pattern in fertilized mouse eggs affects gene expression and development to term. *Dev. Biol.* **300**, 534-544.
Perry, A. C. F. and Verlhac, M.-H. (2008). Second meiotic arrest and exit in frogs and mice. *EMBO Rep.* **9**, 246-251.
Perry, A. C. F., Wakayama, T. and Yanagimachi, R. (1999). A novel *trans*-complementation assay suggests full mammalian oocyte activation is coordinately initiated by multiple, submembrane sperm components. *Biol. Reprod.* **60**, 747-755.
Perry, A. C. F., Wakayama, T., Cooke, I. M. and Yanagimachi, R. (2000). Mammalian oocyte activation by the synergistic action of discrete sperm head components: induction of calcium transients and involvement of proteolysis. *Dev. Biol.* **217**, 386-393.
Peters, J. M. (2002). The anaphase-promoting complex: proteolysis in mitosis and beyond. *Mol. Cell* **9**, 931-943.
Peters, J. M. (2006). The anaphase promoting complex/cyclosome: a machine designed to destroy. *Nat. Rev. Mol. Cell Biol.* **7**, 644-656.
Rauh, N. R., Schmidt, A., Bormann, J., Nigg, E. A. and Mayer, T. U. (2005). Calcium triggers exit from meiosis II by targeting the APC/C inhibitor XErp1 for degradation. *Nature* **437**, 1048-1052.
Reimann, J. D., Freed, E., Hsu, J. Y., Kramer, E. R., Peters, J. M. and Jackson, P. K. (2001a). Emi1 is a mitotic regulator that interacts with Cdc20 and inhibits the anaphase promoting complex. *Cell* **105**, 645-655.
Reimann, J. D., Gardner, B. E., Margottin-Goguet, F. and Jackson, P. K. (2001b). Emi1 regulates the anaphase-promoting complex by a different mechanism than Mad2 proteins. *Genes Dev.* **15**, 3278-3285.
Rickords, L. F. and White, K. L. (1993). Electroporation of inositol 1,4,5-triphosphate induces repetitive calcium oscillations in murine oocytes. *J. Exp. Zool.* **265**, 178-184.
Rogers, N. T., Halet, G., Piao, Y., Carroll, J., Ko, M. S. H. and Swann, K. (2006). The absence of a Ca^{2+} signal during mouse egg activation can affect parthenogenetic preimplantation development, gene expression patterns, and blastocyst quality. *Reproduction* **132**, 45-57.
Runft, L. L., Jaffe, L. A. and Mehlmann, L. M. (2002). Egg activation: where it all begins. *Dev. Biol.* **245**, 237-254.
Schmidt, A., Duncan, P. I., Rauh, N. R., Sauer, G., Fry, A. M., Nigg, E. A. and Mayer, T. U. (2005). *Xenopus* polo-like kinase Plx1 regulates XErp1, a novel inhibitor of APC/C activity. *Genes Dev.* **19**, 502-513.
Shoji, S., Yoshida, N., Amanai, M., Ohgishi, M., Fukui, T., Fujimoto, S., Nakano, Y., Kajikawa, E. and Perry, A. C. F. (2006). Mammalian Emi2 mediates cytostatic arrest and transduces the signal for meiotic exit *via* Cdc20. *EMBO J.* **25**, 834-845.
Stricker, S. A. (1999). Comparative biology of calcium signaling during fertilization and egg activation in animals. *Dev. Biol.* **211**, 157-176.
Tsurumi, C., Hoffmann, S., Geley, S., Graeser, R. and Polanski, Z. (2004). The spindle assemby checkpoint is not essential for CSF arrest of mouse oocytes. *J. Cell Biol.* **167**, 1037-1050.
Tung, J. J., Hansen, D. V., Ban, K. H., Loktev, A. V., Summers, M. K., Adler, J. R., 3rd and Jackson, P. K. (2005). A role for the anaphase-promoting complex inhibitor Emi2/XErp1, a homolog of early mitotic inhibitor 1, in cytostatic factor arrest of *Xenopus* eggs. *Proc. Natl. Acad. Sci. USA* **102**, 4318-4323.
Viiri, K. M., Jänis, J., Siggers, T., Heinonen, T. Y., Valjakka, J., Bulyk, M. L., Mäki, M. and Lohi, O. (2009). DNA-binding and -bending activities of SAP30L and SAP30 are mediated by a zinc-dependent module and monophosphoinositides. *Mol. Cell. Biol.* **29**, 342-356.
Wakayama, T., Perry, A. C. F., Zuccotti, M., Johnson, K. R. and Yanagimachi, R. (1998). Full-term development of mice from enucleated oocytes injected with cumulus cell nuclei. *Nature* **394**, 369-374.
Whitaker, M. J. and Irvine, R. J. (1984). Microinjection of inositol 1,4,5-trisphosphate activates sea urchin eggs. *Nature* **312**, 636-639.
Yamasaki, S., Sakata-Sogawa, K., Hasegawa, A., Suzuki, T., Kabu, K., Sato, E., Kurosaki, T., Yamashita, S., Tokunaga, M., Nishida, K. et al. (2007). Zinc is a novel intracellular second messenger. *J. Cell Biol.* **177**, 637-645.

Yanagimachi, R. (1994). Mammalian fertilization. In *The Physiology of Reproduction*, 2nd edn (ed. E. Knobil and J. D. Neill), pp.189-317. New York: Raven Press.
Yoshida, N. and Perry, A. C. F. (2007). Piezo-actuated mouse intracytoplasmic sperm injection (ICSI). *Nat. Protoc.* **2**, 296-304.
Yoshida, N., Amanai, M., Fukui, T., Kajikawa, E., Brahmajosyula, M., Iwahori, A., Nakano, Y., Shoji, S., Diebold, J., Hessel, H. et al. (2007a). Broad, ectopic expression of the sperm protein, PLCZ1 induces parthenogenesis and ovarian tumours in mice. *Development* **134**, 3941-3952.
Yoshida, N., Brahmajosyula, M., Shoji, S., Amanai, M. and Perry, A. C. F. (2007b). Epigenetic discrimination by mouse metaphase II oocytes mediates asymmetric chromatin remodeling independently of meiotic exit. *Dev. Biol.* **301**, 464-477.